

A Combined Analytic, Numeric, and Experimental Investigation Performed on NiTi/NiTiCu Bi-Layer Composites under Tensile Loading

Milad Taghizadeh, Mahmoud Nili-Ahmadabadi,* Mostafa Baghani, and Mohammad Hassan Malekshoaraei

Adjusting mechanical behavior and controlling deformation parameters are significant tasks in designing shape memory components. In this paper, an analytical model describes the deformation behavior of NiTi/NiTiCu bi-layer composites under tensile loading. Different deformation stages are considered based on single mechanical behavior at each stage. Closed-form equations are derived for stress–strain variations of bi-layer composites under uniaxial loading–unloading. Bi-layer composites made via the diffusion bonding method from single layers of NiTi alloy with a composition of Ti-50.7 at.% Ni, as an austenitic layer, and Ti-45 at.% Ni-5 at.% Cu, as a martensitic layer, are produced by the vacuum arc remelting technique. The tensile behavior of single- and bi-layers is investigated by using loading–unloading experiments to find the nominal stress–strain curves. Numerical simulations are also done by employing Lagoudas constitutive model to simulate stress–strain diagrams. The solutions of the analytical method presented are validated by using the numerical simulations as well as the experimental results. With regard to the results obtained from the analytical modeling, the numerical simulations, and the experiments, it is evident that the bi-layer composites with different thickness ratios provide adjustable mechanical behavior that can be considered in different application designs, for example, actuators equipped with shape memory components.

applications such as actuation mechanisms. The capability of SMAs in shape changing, along the direction of force due to a solid state transformation induced by stress or temperature, can be used in designing actuators. SMAs have low controllability in both thermally and stress-induced transformations; thus, controlling the deformation parameters such as the plateau stress, the transformation, and the pseudo-elastic strain can be an interesting technique to reach adjustable mechanical behavior in the design of SMA components.^[1–4]

Typically, NiTi alloys under tensile loading reveal that large strains take place over a constant value of stress known as Lüders-type deformation.^[5,6] Many parameters such as the amount of cold rolling and the annealing time as well as temperature affect these mechanical properties. However, employing different experimental procedures to improve the properties, results in desirable and different mechanical behaviors to some extent.^[7–10] Moreover, using composite, multi-layered or functionally graded NiTi-based components produces different mechanical characteristics that can be useful in different applications.^[11–15]

1. Introduction

Shape memory alloys (SMAs) as a subgroup of smart materials with two well-known characteristics known as pseudo-elasticity and shape memory effect enjoy a special place on a wide range of

Recently, a bi-layered NiTi thin film deposited on Si substrate exhibited a combined pseudo-elastic behavior and shape memory effect at the same time. Furthermore, thermal hysteresis is also reduced due to its superior properties.^[16] So far, many investigations have been conducted on the analytical modelling of functionally graded NiTi-based components as well as multilayer thin films.^[17–22] Generally, analytical models predict the global response of SMA components under tensile loading and bending. Analytical models are useful tools to predict the mechanical response of SMA components that are capable of reducing difficulties appearing in experimental tests.

More recently, SMAs produced by laser method,^[23–29] have been considered in many applications. In many of these methods, a temperature gradient generated through the laser pulses can control the microstructure of the material resulting in gradient properties which lead to the control of the strain by the stress in the plateaus, and also in controlling the transformation strain. However, controlling the temperature gradient with laser

Prof. M. Nili-Ahmadabadi, M. Taghizadeh,
M. H. Malekshoaraei
School of Metallurgy and Materials Engineering,
College of Engineering, University of Tehran,
Tehran, Iran
E-mail: nili@ut.ac.ir

Prof. M. Nili-Ahmadabadi
Center of Excellence (COE) for High Performance
Materials, School of Metallurgy and Materials
Engineering, University of Tehran, Tehran, Iran

Dr. M. Baghani
School of Mechanical Engineering, College of
Engineering, University of Tehran, Tehran, Iran

DOI: 10.1002/adem.201700395

pulses has its own difficulties and requirements.^[30,31] Another technique employed to adjust the mechanical properties in SMA components is to develop NiTi/NiTiCu bi-layer composites with different thickness ratios that have been made by the diffusion bonding method.^[32] Investigations performed on the diffusion evaluation at the interface of bonding^[33] illustrate that with an increase in the bonding times, the diffusion depth for the components increases, and results in the manufacture of functionally graded SMAs. Moreover, structural parameters such as the thickness ratio affect the mechanical response of the NiTi/NiTiCu bi-layers. In addition to the potential of the NiTi/NiTiCu bi-layer composite manufacturing due to the feasibility of production by diffusion bonding of the single layers, controlling the properties is provided not only by the annealing temperature, but also by the geometrical and structural parameters. For instance, changing the thickness ratios leads to a more handling condition.^[32]

Although several analytical models have been proposed to describe the functionally graded SMAs, to the best knowledge of the authors, there is no analytical model reported in the literature to describe the deformation behavior of the NiTi/NiTiCu bi-layer composites. This paper provides closed-form solutions for stress-strain variations in the NiTi/NiTiCu bi-layer composites under tensile loading-unloading conditions. These solutions are useful for the investigation of the deformation behavior of the NiTi/NiTiCu bi-layer composites with different geometrical and mechanical parameters.

2. Definition of Deformation Parameters

The material parameters for the single-layers of NiTi alloy are defined on the basis of ideal pseudo-elastic and de-twinning responses. **Figure 1a** illustrates the ideal pseudo-elastic behavior in tension; the ideal de-twinning of martensite in tension; and also the ideal de-twinning of the martensite in compression to NiTi SMAs. In **Figure 1a**, σ_M and σ_A are the forward and the reverse transformation stresses, while ε_M and ε_A stand for the forward

and the reverse transformation strains, respectively. The apparent elastic moduli of the austenite is denoted by E_A . In **Figure 1a**, σ_{DTS} and σ_{DTF} are the de-twinning start and finish stresses in tension for the martensitic layer, respectively and ε_{DT} is the de-twinning strain in tension for the martensitic layer. ε_R denotes the residual strain after unloading of the martensitic layer in tension. σ_s and σ_f are the de-twinning start and finish stresses, and ε_{DC} denotes the de-twinning strain in compression to the martensitic layer. α and β show the plateau slope for the martensitic layer in tension and compression, respectively.

Due to the asymmetrical behavior observed in tension-compression and also in loading-unloading for NiTi SMAs,^[34] six different modulus of elasticity were considered for the martensite phase, denoted by E_{M1} to E_{M6} for loading and unloading in tension for both layers and loading in compression to the martensitic layer, respectively as in **Figure 1a**.

Figure 1b shows a NiTi/NiTiCu bi-layer composite of length L , width b , and thickness t . The composite consists of two single layers named A and M, which possess pseudo-elastic and shape memory behavior at room temperature, respectively. Such composites can be produced through the diffusion bonding technique from single-layer sheets, with different thickness ratios in a vacuum furnace. The composite is subjected to a tensile loading F along its length (y-direction).

Figure 2 schematically plots eight different deformation stages based on the ideal mechanical behavior for each layer introduced in **Figure 1a**. It should be noted that in order to reduce complexity in the analysis, it is assumed that the beginning and the end point of each stage precisely match the stress-strain curves at critical points where according to the results observed in the experimental section, under a constant tensile testing temperature for both the single- and the bi-layers, this assumption seems to be reasonable. According to **Figure 2a**, three deformation stages are considered for loading of the bi-layer composite. Due to the complexity of the deformation, in the unloading path while involving the compressive stress in the M layer, five deformation stages are considered for unloading of the bi-layer composite as shown in **Figure 2b**.

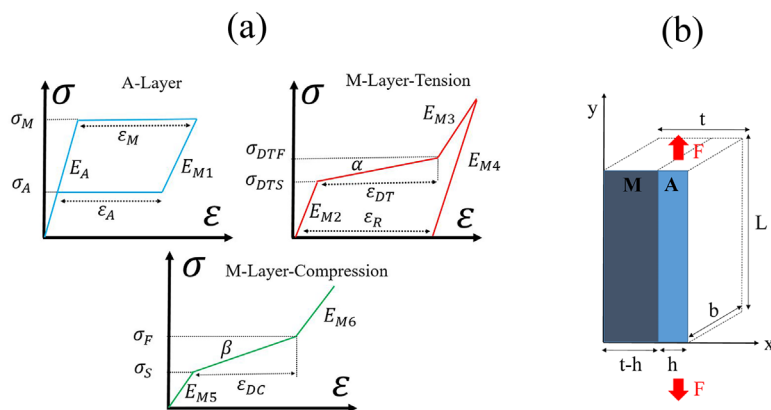


Figure 1. a) Definition of the deformation parameters of the NiTi single layer plate in tension and compression for austenitic layer and martensitic layer, b) geometrical dimensions of the NiTi/NiTiCu bi-layer composite.

3. Developing an Analytical Mathematic Model

In this section, at first, a step to step analytical model is proposed to predict the tensile behavior of the NiTi/NiTiCu bi-layer composites based on some principles of the mechanics of materials, then the capability of the presented model for different structural parameters is investigated and the relevant results are provided.

3.1. Derivation of Closed-Form Stress-Strain Relations for the NiTi/NiTiCu Bi-Layer Composite

This subsection is related to the nominal stress-strain relation development of the NiTi/NiTiCu bi-layer composites. According to **Figure 1b**, the NiTi/NiTiCu

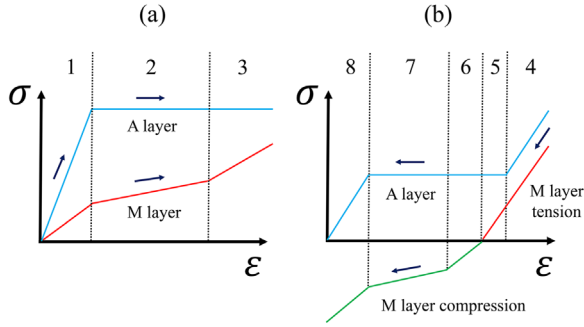


Figure 2. Deformation stages of the NiTi/NiTiCu bi-layer composite for a) loading, b) unloading.

bi-layer composite is loaded along the longitudinal direction. The nominal stress (σ) and strain (ϵ) are then defined as:

$$\sigma = \frac{F}{bt},$$

$$\epsilon = \frac{\Delta L}{L} \quad (1)$$

where L is the initial length of composite and ΔL is the total deformation of the composite in the longitudinal direction. It is assumed that the bi-layer composite remains straight during the loading and subsequent unloading, thus the mode of deformation is iso-strain rather than iso-stress which means both the austenitic and martensitic layers have the same total deformation along the longitudinal direction.

3.1.1. Stage (1) $0 \ll \epsilon < \frac{\sigma_{DT}}{E_{M2}} = \frac{\sigma_M}{E_A}$

At this stage, the A layer is in the austenite phase and the M layer is in the martensite phase. Since the amount of stress is less than the required value to start the stress-induced transformation at the A layer and the de-twinning of the twinned martensite in the M layer, both layers follow Hooke's law; therefore, the nominal stress-strain relation in each layer is

$$\sigma_{Aus} = E_A \cdot \epsilon,$$

$$\sigma_{Mar} = E_{M2} \cdot \epsilon \quad (2)$$

where σ_{Aus} and σ_{Mar} are the nominal stresses for the austenitic and the martensitic layers, respectively. The total load F_t can be found from

$$F_t = F_A + F_M \quad (3)$$

where F_A and F_M are the austenitic layer and the martensitic layer forces, respectively as in Equations. 1 and 2 as

$$F_A = \int \sigma_{Aus} \cdot dA = E_A \cdot \epsilon \cdot b \cdot h,$$

$$F_M = \int \sigma_{Mar} \cdot dA = E_{M2} \cdot \epsilon \cdot b \cdot (t - h) \quad (4)$$

Inserting Equation 4 into 3 and in the light of Equation 1, the nominal stress-strain relation is given as

$$\sigma = \left(E_A \cdot \frac{h}{t} + E_{M2} \cdot \frac{(t-h)}{t} \right) \cdot \epsilon \quad (5)$$

3.1.2. Stage (2) $\frac{\sigma_M}{E_A} \ll \epsilon < \frac{\sigma_M}{E_A} + \epsilon_{DT}$

During this stage, the stress-induced martensitic transformation and the de-twinning of the twinned martensite start within the A and the M layer, respectively; thus, the force in each layer is calculated as follows

$$F_A = \int \sigma_{Aus} \cdot dA = \sigma_M \cdot b \cdot h,$$

$$\begin{aligned} F_M &= \int \sigma_{Mar} \cdot dA = \int \alpha \cdot \left(\epsilon - \left(\frac{\sigma_{DTS}}{E_{M2}} - \frac{\sigma_{DTS}}{\alpha} \right) \right) \cdot dA \\ &= \alpha \cdot \left(\epsilon - \left(\frac{\sigma_{DTS}}{E_{M2}} - \frac{\sigma_{DTS}}{\alpha} \right) \right) \cdot b \cdot (t - h) \end{aligned} \quad (6)$$

Inserting Equation 6 into 3 and using Equation 1, the nominal stress-strain relation is given as

$$\sigma = \left(\frac{\sigma_M \cdot h}{t} + \alpha \cdot \left(\epsilon - \left(\frac{\sigma_{DTS}}{E_{M2}} - \frac{\sigma_{DTS}}{\alpha} \right) \right) \cdot \frac{(t-h)}{t} \right) \quad (7)$$

3.1.3. Stage (3) $\epsilon \gg \frac{\sigma_M}{E_A} + \epsilon_{DT}$

This stage starts when the de-twinning of the twinned martensite ends in the M layer and the de-twinned martensite is in its linear elastic stage, while the stress-induced phase transformation is still ongoing in the A layer. At the end of this stage, the stress-induced phase transformation in the A layer ends and both layers are in the de-twinned martensite phase. Thus, the amount of stress in the M layer is found as

$$\sigma_{Mar} = E_{M3} \left(\epsilon - \left(\epsilon_{DT} + \frac{\sigma_{DTS}}{E_{M2}} - \frac{\sigma_{DTF}}{E_{M3}} \right) \right) \quad (8)$$

Considering Equation 1, the amount of F_A and F_M are recast as

$$F_A = \int \sigma_{Aus} \cdot dA = \sigma_M \cdot b \cdot h,$$

$$\begin{aligned} F_M &= \int \sigma_{Mar} \cdot dA = E_{M3} \cdot \epsilon \cdot b \cdot (t - h) \\ &\quad - E_{M3} \cdot \left(\epsilon_{DT} + \frac{\sigma_{DTS}}{E_{M2}} - \frac{\sigma_{DTF}}{E_{M3}} \right) \cdot b \cdot (t - h) \end{aligned} \quad (9)$$

Inserting Equation 9 into 3 and using Equation 1, the nominal stress-strain relation is given as

$$\begin{aligned} \sigma &= \left(\frac{\sigma_M \cdot h}{t} - \frac{E_{M3} \cdot \left(\epsilon_{DT} + \frac{\sigma_{DTS}}{E_{M2}} - \frac{\sigma_{DTF}}{E_{M3}} \right) \cdot (t-h)}{t} \right) \\ &\quad + \left(\frac{E_{M3} \cdot (t-h)}{t} \right) \cdot \epsilon \end{aligned} \quad (10)$$

Equations 5, 7, and 10 describe the nominal stress–strain relations of the NiTi/NiTiCu bi-layer composite during the tensile loading. As discussed before, because of the complexity of deformation occurring in the unloading path, five deformation stages named (4)–(8) are considered for the unloading of the bi-layer composite.

3.1.4. Stage (4) $\varepsilon \gg \frac{\sigma_A}{E_A} + \varepsilon_A$

This stage is related to the elastic unloading of the de-twinned martensite phase in both layers. This stage ends when the reverse phase transformation starts in the A layer. According to Hook's law, the nominal stress–strain relation in each layer has the following forms

$$\begin{aligned}\sigma_{Aus} &= E_{M1} \left(\varepsilon - \left(\varepsilon_A + \frac{\sigma_A}{E_A} - \frac{\sigma_A}{E_{M1}} \right) \right), \\ \sigma_{Mar} &= E_{M4} (\varepsilon - \varepsilon_R)\end{aligned}\quad (11)$$

With regard to Equation 1, the amounts of F_A and F_M are found as

$$\begin{aligned}F_A &= \int \sigma_{Aus} \cdot dA = E_{M1} \cdot \varepsilon \cdot b \cdot h - E_{M1} \cdot \left(\varepsilon_A + \frac{\sigma_A}{E_A} - \frac{\sigma_A}{E_{M1}} \right) \cdot b \cdot h, \\ F_M &= \int \sigma_{Mar} \cdot dA = E_{M4} \cdot \varepsilon \cdot b \cdot (t - h) - E_{M4} \cdot \varepsilon_R \cdot b \cdot (t - h)\end{aligned}\quad (12)$$

Inserting Equation 12 into 3, with the aid of Equation 1, the nominal stress–strain relation is identified as

$$\begin{aligned}\sigma &= \left(E_{M1} \cdot \frac{h}{t} + E_{M4} \cdot \frac{t-h}{t} \right) \varepsilon \\ &\quad - \left(E_{M1} \cdot \left(\varepsilon_A + \frac{\sigma_A}{E_A} - \frac{\sigma_A}{E_{M1}} \right) \cdot \frac{h}{t} + E_{M4} \cdot \varepsilon_R \cdot \frac{(t-h)}{t} \right)\end{aligned}\quad (13)$$

3.1.5. Stage (5) $\varepsilon_R \ll \varepsilon < \frac{\sigma_A}{E_A} + \varepsilon_A$

During this stage, the reverse transformation from the martensite phase to the austenite phase initiates and progresses at the A layer, while the M layer is still unloaded linearly until the stress vanishes. Thus, the amount of constant stress in the A layer is σ_A and for the M layer it is calculated via Equation 11. Considering Equation 1, the amounts of F_A and F_M are

$$\begin{aligned}F_A &= \int \sigma_{Aus} \cdot dA = \sigma_A \cdot b \cdot h, \\ F_M &= \int \sigma_{Mar} \cdot dA = E_{M4} \cdot \varepsilon \cdot b \cdot (t - h) - E_{M4} \cdot \varepsilon_R \cdot b \cdot (t - h)\end{aligned}\quad (14)$$

Combining Equations 1, 3, and 14, the nominal stress–strain relation is obtained as

$$\sigma = \left(E_{M4} \cdot \frac{(t-h)}{t} \right) \varepsilon + \left(\sigma_A \cdot \frac{h}{t} - E_{M4} \cdot \varepsilon_R \cdot \frac{(t-h)}{t} \right)\quad (15)$$

3.1.6. Stage (6) $\varepsilon_R - \frac{\sigma_s}{E_{M5}} \ll \varepsilon < \varepsilon_R$

At this stage, the M layer goes under compression, while the reverse phase transformation is still governing in the A layer. This stage ends when the M layer reaches the end of the linear elastic deformation limit in compression. The amount of the constant stress in the A layer is σ_A and for the M layer becomes

$$\sigma_{Mar} = E_{M5} (\varepsilon - \varepsilon_R)\quad (16)$$

With regard to Equation 1, the amounts of F_A and F_M are found as

$$\begin{aligned}F_A &= \int \sigma_{Aus} \cdot dA = \sigma_A \cdot b \cdot h, \\ F_M &= \int \sigma_{Mar} \cdot dA = E_{M5} \cdot \varepsilon \cdot b \cdot (t - h) - E_{M5} \cdot \varepsilon_R \cdot b \cdot (t - h)\end{aligned}\quad (17)$$

Inserting Equation 17 into 3 while having Equation 1 in mind, the nominal stress–strain relation is expressed as

$$\sigma = \left(E_{M5} \cdot \frac{(t-h)}{t} \right) \varepsilon + \left(\sigma_A \cdot \frac{h}{t} - E_{M5} \cdot \varepsilon_R \cdot \frac{(t-h)}{t} \right)\quad (18)$$

3.1.7. Stage (7) $\frac{\sigma_A}{E_A} \ll \varepsilon < \varepsilon_R - \frac{\sigma_s}{E_{M5}}$

This stage starts when the linear elastic deformation limit for compression ends in the M layer. Based on previous researches,^[35] unlike the tensile loading, under the compressive loading, the material is quickly strain hardened because of the dislocation generation in both the martensite twin plates and the junction plane areas and thus, no clear stress-plateau is observed. Since the de-twinning is more favored in tension compared to the compression,^[36] it is deduced that in compression, the combination of dislocation generating mechanism and de-twinning influenced the stress–strain curve in the plateau region, while in tension, the de-twinning mechanism is becoming dominant. In this analytical model, the effects of dislocation generation in compression on the plateau slope is considered in β parameter. This stage ends when the de-twinning in compression ends in the M layer. During this stage, the reverse phase transformation is still ongoing in the A layer. The amount of stress for the A layer is σ_A and for the M layer is calculated by

$$\sigma_{Mar} = \beta \left(\varepsilon - \left(\varepsilon_R - \frac{\sigma_s}{E_{M5}} + \frac{\sigma_s}{\beta} \right) \right)\quad (19)$$

Considering Equation 1, the amounts of F_A and F_M are

$$\begin{aligned}F_A &= \int \sigma_{Aus} \cdot dA = \sigma_A \cdot b \cdot h, \\ F_M &= \int \sigma_{Mar} \cdot dA \\ &= \beta \cdot \varepsilon \cdot b \cdot (t - h) - \beta \cdot \left(\varepsilon_R - \frac{\sigma_s}{E_{M5}} + \frac{\sigma_s}{\beta} \right) \cdot b \cdot (t - h)\end{aligned}\quad (20)$$

Inserting Equation 20 into 3 and using Equation 1, the nominal stress–strain relation is recast as

$$\sigma = \left(\beta \cdot \frac{(t-h)}{t} \right) \cdot \varepsilon + \left(\frac{\sigma_A \cdot h}{t} - \beta \cdot \left(\varepsilon_R - \frac{\sigma_s}{E_{M5}} + \frac{\sigma_s}{\beta} \right) \cdot \frac{(t-h)}{t} \right) \quad (21)$$

3.1.8. Stage (8) $0 \ll \varepsilon < \frac{\sigma_A}{E_A}$

This step represents the unloading of the full austenite phase in the A layer and further loading of the de-twined martensite under compression for the M layer. At the end of this stage, the total deformation of the composite returns to zero. Considering Hook's law, the nominal stress–strain relation in each layer is

$$\sigma_{Aus} = E_A \cdot \varepsilon_A,$$

$$\sigma_{Mar} = E_{M6} \left(\varepsilon - \left(\varepsilon_R - \frac{\sigma_s}{E_{M5}} - \varepsilon_{DC} + \frac{\sigma_f}{E_{M6}} \right) \right) \quad (22)$$

Employing Equation 1, the amounts of F_A and F_M are

$$F_A = \int \sigma_{Aus} \cdot dA = E_A \cdot \varepsilon \cdot b \cdot h,$$

$$F_M = \int \sigma_{Mar} \cdot dA = E_{M6} \cdot \varepsilon \cdot b \cdot (t-h) - E_{M6} \cdot \left(\varepsilon_R - \frac{\sigma_s}{E_{M5}} - \varepsilon_{DC} + \frac{\sigma_f}{E_{M6}} \right) \cdot b \cdot (t-h) \quad (23)$$

Inserting Equation 23 into 3, and employing Equation 1, the nominal stress–strain relation is given by

$$\sigma = \left(E_A \cdot \frac{h}{t} + E_{M6} \cdot \frac{t-h}{t} \right) \varepsilon - \left(E_{M6} \cdot \left(\varepsilon_R - \frac{\sigma_s}{E_{M5}} - \varepsilon_{DC} + \frac{\sigma_f}{E_{M6}} \right) \cdot \frac{t-h}{t} \right) \quad (24)$$

Equations 5, 7, 10, 13, 15, 18, 21, and 24 describe the nominal stress–strain relation of the NiTi/NiTiCu bi-layer composite at the deformation stages defined in Stages (1)–(8).

3.2. Analytical Model Predictions for the NiTi/NiTiCu Bi-Layer Composite

Figure 3a shows the nominal stress–strain plot of a NiTi/NiTiCu bi-layer composite with 2:1 (M:A) ratio under uniaxial tensile loading, employing the close-form solution derived from the preceding section with the material parameters listed in Table 1. It should be point out that the material parameter identification method for the data given in Table 1 is expressed in the following experimental section. The dash-line curve in Figure 3a is the

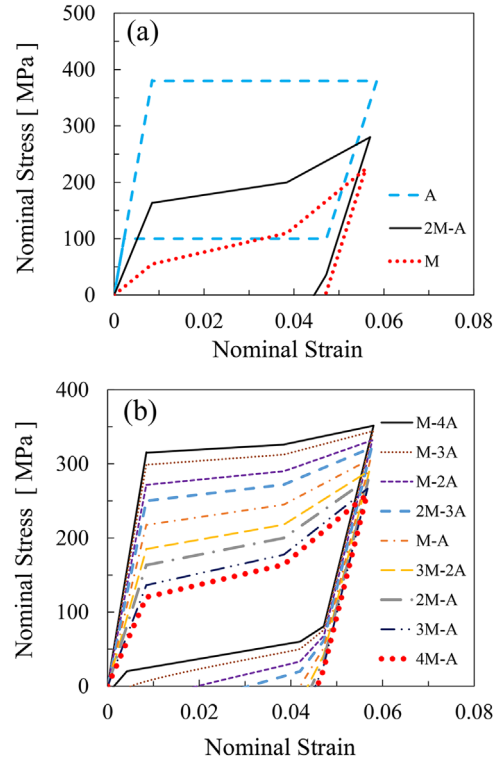


Figure 3. Analytical model predictions for the nominal stress–strain diagrams for the NiTi/NiTiCu bi-layer composite: a) compared to the single layers, b) different thickness ratios of A–M.

stress–strain behavior of the single A layer, and the dot-line is related to the stress–strain behavior of the single M layer. The solid line is related to the stress–strain behavior of the NiTi/NiTiCu bi-layer composite. As seen in Figure 3a, the stress–strain curve for the NiTi/NiTiCu bi-layer composite lies between the A and the M layer stress–strain curves and the plateau stress for the composite follows the rule of mixtures. The transformation strain for the bi-layer sample is smaller than that of the A layer and is larger than the de-twining strain of the M layer.

Figure 3b depicts the nominal stress–strain diagrams of nine bi-layer composites with different A to M thickness ratios. As one may observe from Figure 3b, a change in thickness ratios, results in a change in the stress–strain diagrams. Larger values of A to M thickness ratio lead to an increase in the stress plateau as well as in the pseudo-elastic strain. Consequently, employing different A to M ratios results in various transformation strains. Thus, the NiTi/NiTiCu bi-layer composites with different thickness ratios provide adjustable mechanical behaviors that are useful in the design procedure of structures with SMA components.

It should be noted, in order to avoid a significant amount of dislocation generation and maintain the shape memory property,^[37] it is more appropriate that the M layer does not experience the compression after tension. For this purpose, the thickness ratio should be considered in such a way that the M layer does not go under compression. The critical value of the thickness ratio to prevent the M layer from entering the compression stage can be achieved by equalizing the force relationship of the layers. For this purpose, in stage 7, by dividing

Table 1. Material properties of the NiTi/NiTiCu bi-layer composite.

σ_M [MPa]	σ_A [MPa]	ε_M	ε_A	ε_{DT}	ε_{DC}	ε_R	σ_s [MPa]	σ_f [MPa]	α [GPa]
380	100	0.050	0.045	0.030	0.028	0.047	100	240	1.83
E_A [GPa]	E_{M1} [GPa]	E_{M2} [GPa]	E_{M3} [GPa]	E_{M4} [GPa]	E_{M5} [GPa]	E_{M6} [GPa]	σ_{DTS} [MPa]	σ_{DTF} [MPa]	β [GPa]
45	25	6.5	6.5	25	20	20	55	110	5

σ_s by σ_A , the critical value of the thickness ratio is equal to 1. Thus, for the A/M thickness ratios less than 1 ($t - h > h$), the M layer does not experience the compressive behavior in the unloading of the composite.

4. Experimental Section

To validate the analytical solutions proposed in the previous section, the A layer with Ni-rich Ti-50.7at%Ni composition and the M layer with Cu-included Ti-rich, Ti-45at%Ni-5at%Cu composition were prepared by alloying and using a vacuum arc melting furnace followed by forging, solution annealing, and also hot and cold rolling to reach the desirable thicknesses (0.6 mm for tensile and 3 mm for compressive specimens). At this step, the sheets that are supposed to be used for the single layers and compressive samples, experience the final 30-min annealing at 500 °C to improve the shape memory and superelasticity characteristics. Also, X-ray Diffraction (XRD) analysis of the bulk samples are performed using Cu-K α to recognize the room temperature phases with the scan speed of 0.125° min⁻¹ from 30° to 50° as shown in **Figure 4a**. The solid line related to the austenitic sample illustrates only the austenite peak where the diffraction pattern of the martensitic sample (dashed line) shows the martensite phase peaks. In other words, the A and the M layer samples contain fully austenite and fully martensite phases in ambient temperature, respectively.

For the bi-layer samples, sheets of specimen A and M with a dimension of 2 × 1 mm² were ground by 400, 800, 1200, 2000,

and 4000 grit SiC papers and polished by means of a 40-nm colloidal Alumina suspension. Layers with 3:1 and 2:1 ratio ($M:A$) were bonded under diffusion bonding process in a vacuum tube furnace at 1000 °C for 3 h and under 20 MPa compressive stress applied by a super alloy fixture as schematically shown in **Figure 4b**. Afterwards, 20% rolling followed by a final 30-min annealing at 500 °C was conducted on the bonded layers to improve the shape memory and superelasticity characteristics. The experimental results and theoretical calculations obtained from the analysis of line scan and the diffusion equation under the above annealing condition, confirmed that the diffusion depths for Ni and Cu were about 30 and 15 μ m, respectively, also the SEM images from the interface of bonding confirmed that the A and the M layers were still in their initial phase.^[32,33] Although the interface of bonding could affect the mechanical behavior of the NiTi/NiTiCu bi-layers, with regard to the total thickness of composite, the fraction of concentration gradient area under above annealing condition is negligible (≈ 0.05); so, it is assumed that the A and the M layers maintain their full pseudo-elastic and full de-twinning properties after the diffusion bonding.

Tensile and Compressive samples were prepared through the electric discharge machining. The gauge length of the single layer tensile samples was 30 mm. Compressive test samples were 2 mm in diameter and 2.4 mm in height. The gauge length of the bi-layer tensile samples was 10 mm.

Tensile behavior of the single-layers as well as the bi-layers was investigated by using a two-step method with the strain rate of 2.8×10^4 s⁻¹. At the first step, samples were loaded up to certain amounts of displacement and at the second step, the displacement was set to zero. Moreover, the compressive behavior of the M layer was investigated for those stages requiring compressive behaviors under the same condition and strain rate. The nominal stress–strain curves of the single-layers for the tensile and compressive behavior as well as the bi-layers for tensile behavior are measured.

Thermal recovery of strain for the bi-layers was investigated by using a three-step method. At the first step, samples were loaded up to a certain amount of force. At the second step, the force was set to zero until the bi-layer composite was fully unloaded. At the third step and after a 10-s delay, the samples were heated through an electric current for 30 s by connecting wires to their ends. The thermal strain recovered for both specimens with two different thickness ratios, was measured for a period of 30 s.

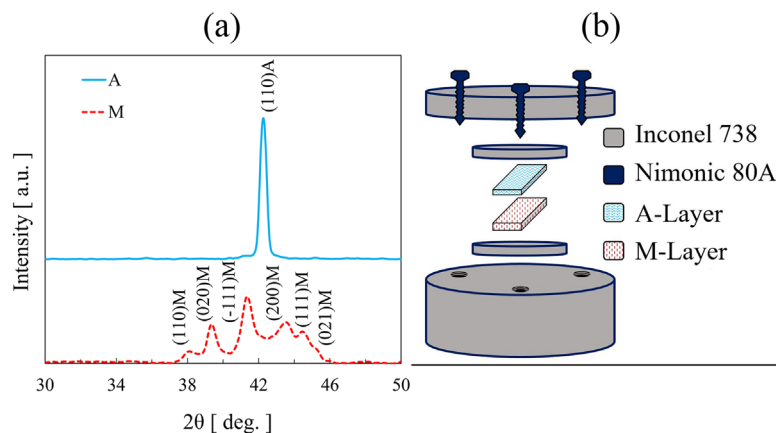


Figure 4. a) XRD patterns for the A and M layer of the NiTi alloy used in experiments, b) exploded view drawing for super alloy fixture used in sample construction stage.

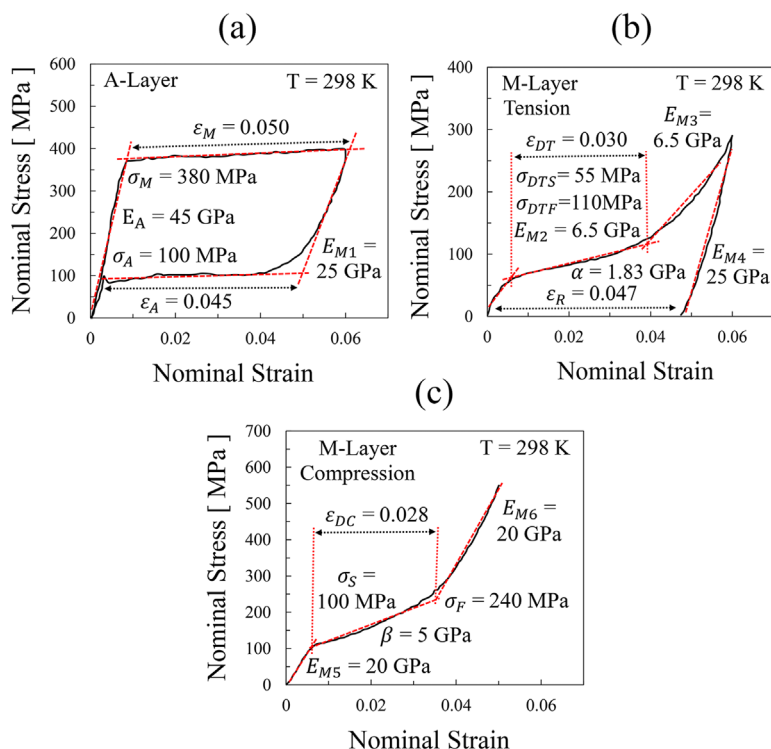


Figure 5. Experimental stress–strain diagrams of the NiTi single layers under uniaxial loading; a) the austenitic layer under tension; b) the martensitic layer under tension; and c) the martensitic layer under compression.

Experimental Tensile and Compressive Tests on the NiTi Single Layers: **Figure 5a** shows the full superelastic behavior under 6% tensile strain for the A layer. Because of the stress-induced phase transformation and with the application of stress, the martensite becomes more stable, but as the stress is unloaded, the martensite phase experiences instability. The upper plateau represents the formation of martensite phase under stress, while the lower plateau manifests the reversion of the SIM leading to the formation of the austenite phase when the stress is released. Since only one martensite variant is formed under the stress, there is a significant shape change which is fully recovered upon the release of the stress after a certain amount of strain.^[38]

Figure 5b illustrates the de-twinning process for the twinned martensite taking place in the M layer under 6% tensile strain which results in the appearance of the stress plateau in the stress–strain curves. Experimental results reveal that, at the testing temperatures below the austenite start temperature (A_s), a stress-plateau is observed under the tensile deformation. With the application of further deformation beyond the stress-plateau, more reorientation, and de-twinning of the martensite twins occur, that are less favorable to the applied stress. In this area, the deformation of martensite twins goes along with a further rise in the applied force.^[39]

Figure 5c shows the stress–strain diagram of the martensitic layer under uniaxial compressive loading. According to **Figure 5b**, there is asymmetrical behavior in the tension and compression as previously reported in, for example.^[35] As mentioned in Section 3, unlike the tensile loading, under the compressive loading, the material is quickly strain-hardened,

and no observable stress-plateau exists. Employing the experimental data plotted in **Figure 5**, the transformation and material properties of the NiTi/NiTiCu bi-layer composite were calibrated as tabulated in Table 1. For this purpose, a number of dashed lines were tangent to the stress–strain curves of the single layers and the material parameters were calculated through measuring the length and slopes of the dashed lines.

Experimental Tensile Tests on the NiTi/NiTiCu Bi-Layers: **Figure 6a** shows the stress–strain diagram of the NiTi/NiTiCu bi-layer composites under uniaxial tensile loading. As shown in **Figure 6a**, similar to the predictions made by the analytical model in the previous sections, increasing the A–M thickness ratio, increases the stress plateau and the pseudo-elastic strain to the higher levels, and therefore results in the higher transformation strains. Furthermore, considering the stress plateaus shown in **Figure 5**, for both the A and the M layer in tension, the stress plateau for the NiTi/NiTiCu bi-layer composites lies between the stress plateaus experimentally observed in the single layers.

Figure 6b shows the diagram of thermal recovery of the strain versus time. As shown in **Figure 6b**, the remaining strain shown in **Figure 6a** is fully recovered by heating the samples due to the shape memory properties of the M layer. It is also observed that the amount of the recovered strain is increased for the 3:1 (M:A) thickness ratio that confirms that as the amount of the M layer increases, the amount of the shape memory strain grows and consequently the amount of pseudoelastic strain decreases. This behavior could be observed by the slope changes at the unloading stage in the stress–strain diagrams shown in **Figure 6a**. This

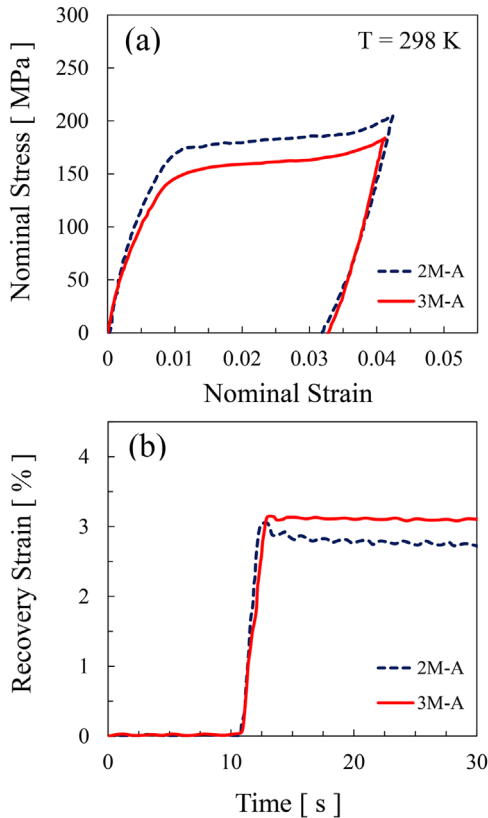


Figure 6. a) The experimental tensile stress–strain diagram of the NiTi/NiTiCu bi-layer composites under uniaxial loading, b) thermal recovery of the bi-layers after loading-unloading tensile test.

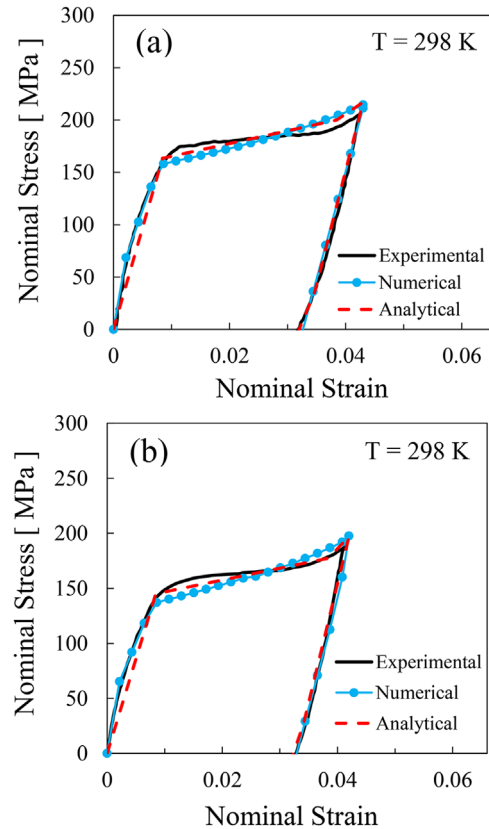


Figure 7. The nominal stress–strain curves of the NiTi/NiTiCu bi-layer composites under uniaxial tensile loading; a) 2:1 ratio ($M:A$), b) 3:1 ratio ($M:A$).

means that changing the thickness ratio in the bi-layer composites, the stress and the strain of the plateau and also the shape memory and pseudo-elastic strain can be adjusted to arrive at the desirable values.

It should be noted that due to the asymmetry of the structure after unloading the composites provided, a small bent toward the austenitic layer which was previously reported is observed.^[18,32]

Comparison of the Analytical Model Predictions with the Experiments and FEM Studies: By introducing the parameters defined in Table 1 into the set of stress–strain formulations proposed in Section 3, the stress–strain response of the NiTi/NiTiCu bi-layer composite is analytically predicted for two thickness ratios.

FEM studies were conducted using the constitutive model developed by Lagoudas et al.^[40] through a user-defined subroutine UMAT in conjunction with constitutive behavior definition in ABAQUS for simulating the stress–strain

diagrams. The material parameters required by the SMA_UM subroutine are Young’s moduli of both austenite and martensite (E_A and E_M); the martensite start and finish and the austenite start and finish temperatures (M_s, M_f, A_s , and A_f , respectively); the maximum transformation strain (H); and the austenite and martensite stress influence coefficients ($\rho\Delta s^A$ and $\rho\Delta s^M$, respectively). These material parameters are shown in Table 2 calculated by using the stress–strain curve data extracted from Figure 5. The NiTi/NiTiCu bi-layer composites with different thickness ratios were designed and numerically analyzed in ABAQUS Software. For overall comparison, the results of the experimental tests, FEM studies, and analytical model are shown in Figure 7. It is observed that the analytical model predictions are in a good agreement with the experimental observations as well as with the FEM studies.

Figure 8 illustrates the effects of changing A/M ratio on the plateau stress and strain of the NiTi/NiTiCu bi-layer composites

Table 2. Lagoudas constitutive model parameters used in the FEM analysis for the NiTi/NiTiCu bi-layer composite

Properties	E_A [GPa]	E_M [GPa]	H	Dimension		M_s [K]	M_f [K]	A_s [K]	A_f [K]
				$\rho\Delta s^A$ [Pa K ⁻¹]	$\rho\Delta s^M$ [Pa K ⁻¹]				
A layer	45	25	0.045	-32143	-108917	175	133	192	223
M layer	45	15	0.047	-2350000	-1292500	330	316	334	347

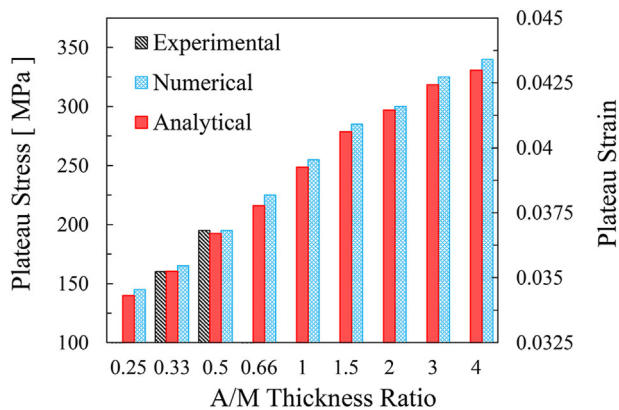


Figure 8. The effects of changing the thickness ratio on the plateau stress and strain of the NiTi/NiTiCu bi-layer composite.

obtained from the analytical and FEM methods. In order to validate the results of the analytical modeling and simulations, the experimental results of the plateau stress and strain of composites with two thickness ratios are presented in Figure 8. With regard to the results of the analytical modelling, FEM study, and experimental tests, it is evident that the bi-layer composites with different thickness ratios show different deformation parameters; varying the relative thickness of the layers leads to more handling condition that can be considered in designing SMA components.

5. Summary and Conclusions

- 1) NiTi/NiTiCu bi-layer composites consisting of austenitic and martensitic layers with different thickness ratios are produced by the diffusion annealing at 1000 °C and 20 MPa compressive stress for 3 h in a vacuum furnace. In order to improve the pseudo-elasticity and shape memory properties, the samples were cold rolled and annealed at 500 °C for 0.5 h in a vacuum furnace. The bi-layer composites show adjustable behavior and varying the relative thickness of the layers results in varying plateau stress and strain and also shape memory and pseudoelastic strain.
- 2) An analytical model is proposed to describe the deformation behavior of the NiTi/NiTiCu bi-layer composites during uniaxial tensile loading–unloading and the closed-form equations are derived for the nominal stress–strain variations. FEM studies are conducted using Lagoudas 3D constitutive model implemented in a user-subroutine UMAT in conjunction with constitutive behavior definition in ABAQUS for simulating the stress–strain diagrams. The model shows a good agreement with both the experimental and FEM results.
- 3) Increasing the A/M thickness ratio in the NiTi/NiTiCu bi-layer composites increases the stress plateau, the transformation, and the pseudo-elastic strain to higher levels, while decreasing the shape memory strain. Therefore, the NiTi/NiTiCu bi-layer composites with different thickness ratios

provide a combination of adjustable mechanical behaviors that can be considered in the design of SMA components.

Conflict of Interest

The authors declare no conflict of interest.

Keywords

shape memory alloys, bi-layer composite, simulation, analytical modeling, FEM study

Received: May 1, 2017

Revised: July 26, 2017

Published online:

- [1] J.A. Shaw, S. Kyriakides, *Acta Mater.* **1997**, 45, 683.
- [2] Y. Bellouard, *Mater. Sci. Eng. A* **2008**, 481, 582.
- [3] J. Van Humbeeck, *Mater. Sci. Eng. A* **1999**, 273, 134.
- [4] F. Reading, *Sci. Bus. Media, LLC* **1998**, 1144.
- [5] G. Tan, Y. Liu, P. Sittner, M. Saunders, *Scr. Mater.* **2004**, 50, 193.
- [6] P. Sittner, Y. Liu, V. Novak, *J. Mech. Phys. Solids* **2005**, 53, 1719.
- [7] H. Shahmir, M. Nili-Ahmadabadi, Y. Huang, J. M. Jung, H. S. Kim, T. G. Langdon, *Mater. Sci. Eng. A* **2015**, 626, 203.
- [8] H. Shahmir, M. Nili-Ahmadabadi, C. T. Wang, J. M. Jung, H. S. Kim, T. G. Langdon, *Mater. Sci. Eng. A* **2015**, 629, 16.
- [9] E. Sharifi, A. Kermanpur, F. Karimzadeh, *Mater. Sci. Eng. A* **2014**, 607, 33.
- [10] L. A. Vieira, F. M. B. Fernandes, R. M. Miranda, L. Quintino, A. Cuesta, *Mater. Sci. Eng. A* **2011**, 528, 5560.
- [11] E. Wang, Y. Tian, Z. Wang, F. Jiao, C. Guo, F. Jiang, *J. Alloys Compd.* **2017**, 696, 1059.
- [12] M. Mohri, M. Nili-Ahmadabadi, M. PouryazdanPanah, H. Hahn, *Mater. Sci. Eng. A* **2016**, 668, 13.
- [13] M. Mohri, M. Nili-Ahmadabadi, *Adv. Eng. Mater.* **2015**, 103, 75.
- [14] M. Mohri, M. Nili-Ahmadabadi, *Sensors Actuators, A Phys.* **2015**, 228, 151.
- [15] M. F. Razali, A. S. Mahmud, *J. Alloys Compd.* **2015**, 618, 182.
- [16] M. Mohri, M. Nili-Ahmadabadi, J. Ivanisenko, R. Schwaiger, H. Hahn, V. S. K. Chakravadhanul, *Thin Solid Films* **2015**, 583, 245.
- [17] A. Ishida, *Sensors Actuators, A Phys.* **2015**, 222, 228.
- [18] B. S. Shariat, Y. Liu, Q. Meng, G. Rio, *Acta Mater.* **2013**, 61, 3411.
- [19] B. S. Shariat, Y. Liu, G. Rio, *J. Alloys Compd.* **2012**, 541, 407.
- [20] B. S. Shariat, Y. Liu, G. Rio, *Smart Mater. Struct.* **2013**, 22.
- [21] B. S. Shariat, Y. Liu, G. Rio, *J. Alloys Compd.* **2013**, 577, S76.
- [22] B. S. Shariat, Y. Liu, G. Rio, *Intermetallics* **2014**, 50, 59.
- [23] A. Shelyakov, N. Sitnikov, K. Borodako, A. Menushenkov, V. Fominski, *Phys. Procedia* **2015**, 73, 108.
- [24] X. Wang, Z. Xue, J. J. Vlassak, Y. Bellouard, in *SMST 2006 Proc. Int. Conf. SHAPE Mem. SUPERELASTIC Technol.* **2008**, 331.
- [25] A. V. Shelyakov, N. N. Sitnikov, D. V. Sheyfer, K. A. Borodako, A. P. Menushenkov, V. Y. Fominski, *Smart Mater. Struct.* **2015**, 24, 115031.
- [26] A. Pequegnat, B. Pantan, Y. N. Zhou, M. I. Khan, *Mater. Des.* **2016**, 92, 802.
- [27] S. Shiva, I. Palani, C. Paul, B. Singh, *Proc. Inst. Mech. Eng. Part B J. Eng. Manuf.* **2016**.
- [28] A. J. Birnbaum, G. Satoh, Y. L. Yao, *J. Appl. Phys.* **2009**, 106, 043504.

- [29] T. E. Abioye, P. K. Farayibi, P. Kinnel, A. T. Clare, *Int. J. Adv. Manuf. Technol.* **2015**, 79, 843.
- [30] Q. Meng, Y. Liu, H. Yang, T. H. Nam, *Scr. Mater.* **2011**, 65, 1109.
- [31] Q. Meng, Y. Liu, H. Yang, B. S. Shariat, T. H. Nam, *Acta Mater.* **2012**, 60, 1658.
- [32] M. H. Malekshoaraei, M. Nili-Ahmadabadi, in *Int. Conf. Mater. Chain From Discov. to Prod.*, **2016**.
- [33] M. Mohri, M. Nili-Ahmadabadi, S. Flege, *J. Alloys Compd.* **2014**, 594, 87.
- [34] P. Sittner, L. Heller, J. Pilch, C. Curfs, T. Alonso, D. Favier, *J. Mater. Eng. Perform.* **2014**, 23, 2303.
- [35] Y. Liu, Z. Xie, J. Van Humbeeck, L. Delaey, *Acta Mater.* **1998**, 46, 4325.
- [36] K. Gall, H. Sehitoglu, Y. I. Chumlyakov, I. V Kireeva, *Acta Mater.* **1999**, 47, 1203.
- [37] Z. Xie, Y. Liu, J. Van Humbeeck, *Acta Mater.* **1998**, 46, 1989.
- [38] T. W. Duerig, K. N. Melton, D. Stoeckel, C. M. Wayman, D. Stockel, *Engineering Aspects of Shape Memory Alloys*, Butter worth-Heinemam, London, **1990**.
- [39] Y. Liu, Z. Xie, *Detwinning in Shape Memory Alloy*, Nova Science Publishers Inc., Hauppauge, New York **2007**.
- [40] D. Lagoudas, Z. Bo, M. A. Qidwai, P. B. Entchev, *SMA UM: User Material Subroutine for Thermomechanical Constitutive Model of Shape Memory Alloys*, Texas A&M University College Station TX, Texas **2003**.